Over-expression of the RieskeFeS protein increases electron transport rates and yield in *Arabidopsis*

Andrew J. Simkin[2], Lorna McAusland[3], Tracy Lawson[2], and Christine A. Raines[2]*

[1] This work was supported by the Biotechnology and Biological Sciences Research Council (Grant: BB/J004138/1 awarded to C.A.R and T.L)

[2] School of Biological Sciences, Wivenhoe Park, University of Essex, Colchester, CO4 3SQ, UK.[3] current address: Division of Crop and Plant Science, School of Biosciences, University of Nottingham LE12 5RD, UK.

* Address correspondence to C.A. Raines. rainc@essex.ac.uk

A.J.S generated transgenic plants and performed molecular and biochemical experiments and carried out plant phenotypic and growth analysis. A.J.S and L.M performed gas exchange measurement on Arabidopsis. A.J.S and L.M carried out data analysis on their respective contributions. C.R and T.L designed and supervised the research. C.R, A.J.S wrote the manuscript with input from TL.

Short title: Enhanced electron transport improves yield

One-sentence summary: Over-expression of the Rieske FeS protein results in significant increases in the quantum efficiencies or PSI and PSII, increases in A_{max} and has the potential to increase crop productivity

Abstract

In this study we have generated transgenic Arabidopsis plants over-expressing the Rieske FeS protein (PetC), a component of the cytochrome b_6f (cyt b_6f) complex. Increasing the levels of this protein, resulted in the concomitant increase in the levels of cyt *f* (PetA) and cyt b_6 (PetB), core proteins of the cyt b_6f complex. Interestingly, an increase in the levels of proteins in both the PSI and PSII complexes was also seen in the Rieske FeS ox plants. Although the mechanisms leading to these changes remain to be identified, the transgenic plants presented here provide novel tools to explore this. Importantly, the overexpression of the Rieske FeS protein resulted in a substantial and significant impact on the quantum efficiency of PSI and PSII, electron transport, biomass and seed yield in Arabidopsis plants. These results demonstrate the potential for manipulating electron transport processes to increase crop productivity.

Keywords: Electron transport, photosynthetic pigments, thylakoid membrane, cytochrome b_6f complex, seed yield

Introduction

Increasing food and fuel demands by the growing world population has led to the need to develop higher yielding crop varieties (Fischer and Edmeades, 2010; Ray et al., 2012). Transgenic studies, modelling approaches and theoretical considerations provide evidence that increasing photosynthetic capacity is a viable route to increase the yield of crop plants (Zhu et al., 2010; Raines, 2011; Long et al., 2015; von Caemmerer and Furbank, 2016). There is now a growing body of experimental evidence showing that increasing the levels of photosynthetic enzymes in carbon metabolism, results in increased photosynthesis and plant biomass (Miyagawa et al., 2001; Raines, 2006, 2011; Lefebvre et al., 2005; Rosenthal et al., 2011; Uematsu et al., 2012; Simkin et al., 2015, 2017; Driever et al., 2017). In addition, manipulation of photosynthetic electron transport by introduction of the algal cytochrome c6 protein has been shown to improve the efficiency of photosynthesis and to stimulate plant growth in low light (Chida et al., 2007). One endogenous target identified for manipulation is the cytochrome b_6f (cyt b_6f) complex which is located in the thylakoid membrane and functions in both linear and cyclic electron transport, providing ATP and NADPH for photosynthetic carbon fixation. Initially, cyt b_6f inhibitors (Kirchhoff et al., 2000) and later transgenic antisense studies suppressing the accumulation of the Rieske FeS protein (PetC), a component of the cyt b_6f complex, have demonstrated that the activity of the cyt b_6f complex is a key determinant of the rate of electron transport (Price et al., 1995, 1998; Anderson et al., 1997; Ruuska et al., 2000; Yamori et al., 2011a,b).

The finding that the cyt b_6f complex is a potential limiting step in the electron transport chain suggests that by increasing the activity of this complex it may be possible to increase the rate of photosynthesis. However, questions have been raised about the feasibility of manipulating this multiprotein, membrane located, complex given that it is composed of eight different subunits, six being encoded in the chloroplast genome (PetA (cyt f), PetB (cyt b_6),

PetD, PetG, PetL and PetN) and two in the nucleus (PetC, (Rieske FeS) and PetM) (Willey and Grey, 1988; Anderson et al., 1992; Knight et al., 2002; Cramer & Zhang, 2006, Cramer et al., 2006; Baniulis et al., 2009; Schöttler et al., 2015). Furthermore, this protein complex functions as a dimer with the transmembrane domains of both the Rieske FeS and cyt b_6 proteins being directly implicated in the monomer–monomer interaction and stability of the complex and the *petD* gene product functioning as a scaffold (Hager et al., 1999; Schwenkert et al., 2007; Hojka et al., 2014; Cramer et al., 2006). Essential roles in the assembly and stability of the cyt b_6f complex have also been shown for the PetG, PetN and PetM subunits and a minor role in stability assigned to the PetL gene product (Schöttler et al., 2007; Bruce and Malkin, 1991; Kuras and Wollman, 1994; Hager et al., 1999; Monde et al., 2000; Schwenkert et al., 2007; Hojka et al., 2014).

Notwithstanding both the genetic and structural complexity of the cyt b_6f complex, it has been shown previously that it is possible to manipulate the levels of the cyt b_6f complex by down regulation of the expression of the Rieske FeS protein (Price. et al., 1998; Yamori et al., 2011a). It has also been shown that the Rieske FeS protein is one of the subunits required for the successful assembly of the cyt b_6f complex (Miles, 1982; Metz et al., 1983; Barkan et al., 1986; Anderson et al., 1997). Based on these results, we reasoned that over-expression of the Rieske FeS protein could be a feasible approach to take in order to increase the electron flow through the cyt b_6f. In this paper we report on the production of Arabidopsis with increased levels of the tobacco Rieske FeS protein and we show that this manipulation resulted in an increase in photosynthetic electron transport, CO_2 assimilation and yield. This work provides evidence that the process of electron transport is potential route for the improvement of plant productivity.

Material and methods

Rieske iron sulphur protein of the cytochrome b_6f (*cyt* b_6f)

The full-length coding sequence of the Rieske iron sulphur protein of the cytochrome b_6f (X64353) was amplified by RT-PCR using primers NtRieskeFeSF (5'caccATGGCTTCTTCTACTCTTTCTCCAG'3) and NtRieskeFeSR (5'CTAAGCCCACCATGGATCTTCACC'3). The resulting amplified product was cloned into pENTR/D (Invitrogen, UK) to make pENTR-*NtRieskeFeS* and the sequence was verified and found to be identical. The full-length cDNA was introduced into the pGWB2 gateway vector (Nakagawa et al., 2007: AB289765) by recombination from the pENTR/D vector to make pGW-NtRieske (B2-NtRi). cDNA are under transcriptional control of the 35s tobacco mosaic virus promoter, which directs constitutive high-level transcription of the transgene, and followed by the *nos* 3' terminator. Full details of the B2-NtRi construct assembly can be seen in Supplemental **Fig. S1.**

Generation of transgenic plants

The recombinant plasmid B2-NtRi was introduced into wild type Arabidopsis by floral dipping (Clough and Bent, 1998) using *Agrobacterium tumefaciens* GV3101. Positive transformants were regenerated on MS medium containing kanamycin (50mg L^{-1}), hygromycin (20mg L^{-1}). Kanamycin/hygromycin resistant primary transformants (T1 generation) with established root systems were transferred to soil and allowed to self-fertilize.

Plant Growth Conditions

Wild type T2 Arabidopsis plants resulting from self-fertilization of transgenic plants were germinated in sterile agar medium containing Murashige and Skoog salts, selected on kanamycin and grown to seed in soil (Levington F2, Fisons, Ipswich, UK) and lines of

121 interest were identified by western blot and qPCR. For experimental study, T3 progeny seeds
122 from selected lines were germinated on soil in controlled environment chambers at an
123 irradiance of 130 µmol m^{-2} s^{-1} in an 8 h/16 h square-wave photoperiod, with an air
124 temperature of 22°C and a relative humidity of 60%. Plants position was randomised and the
125 position of the trays rotated daily under the light. Leaf areas were calculated from
126 photographic images using ImageJ software (imagej.nih.gov/ij). Wild type plants used in this
127 study were a combined group of WT and null segregants from the transgenic lines, verified
128 by PCR for non-integration of the transgene, as no significant differences in growth
129 parameters were seen between them (Supplemental **Fig. S2**).
130
131 **Protein Extraction and Immunoblotting**
132 Four leaf discs (0.6-cm diameter) from two individual leaves were taken, immediately
133 plunged into liquid N^2 and subsequently stored at -80°C. Samples were ground in liquid
134 nitrogen and protein quantification determined (Harrison et al., 1998). Samples were loaded
135 on an equal protein basis, separated using 12% (w/v) SDS-PAGE, transferred to
136 polyvinylidene difluoride membrane, and probed using antibodies raised against the
137 cytochrome *b_6f complex* proteins cyt *f* (PetA: (AS08306), cyt *b_6* (PetB: (AS03034), Rieske
138 FeS (PetC: AS08330), the photosystem I Lhca1 (AS01005) and PsaA (AS06172) proteins the
139 Photosystem II PsbA/D1 (AS01016) and PsbD/D2 (AS06146) proteins, ATP synthase delta
140 subunit (AS101591), and against the glycine decarboxylase H-subunit (AS05074), all
141 purchased from Agrisera (via Newmarket Scientific UK). FBPA antibodies were raised
142 against a peptide from a conserved region of the protein [C]-ASIGLENTEANRQAYR-
143 amide, Cambridge Research Biochemicals, Cleveland, UK (Simkin et al., 2015). Proteins
144 were detected using horseradish peroxidase conjugated to the secondary antibody and ECL
145 chemiluminescence detection reagent (Amersham, Buckinghamshire, UK). Proteins were

146 quantified using a Fusion FX Vilber Lourmat imager (Peqlab, Lutterworth, UK) as previously
147 described (Vialet-Chabrand et al., 2017).
148
149 **Chlorophyll Fluorescence Imaging**
150 Chlorophyll fluorescence measurements were performed on 10-day-old Arabidopsis
151 seedlings that had been grown in a controlled environment chamber at a photosynthetic
152 photon flux density (PPFD) of 130 µmol $m^{-2}s^{-1}$ ambient CO_2 at 22°C. Images of the operating
153 efficiency of photosystem two (PSII) photochemistry, (F_q'/F_m') were taken at PPFDs of 310
154 and 600 µmol m^{-2} s^{-1} using a chlorophyll fluorescence imaging system, (Technologica,
155 Colchester, UK; Barbagallo et al., 2003; Bakerand Rosenqvist, 2004). F_q'/F_m', was
156 calculated from measurements of steady state fluorescence in the light (F') and maximum
157 fluorescence in the light (F_m') was obtained after a saturating 800 ms pulse of 6200 µmol m^{-2}
158 s^{-1} PPFD using the following equation $F_q'/F_m' = (F_m'-F')/F_m'$. (Baker et al., 2001;
159 Oxborough and Baker 1997a).
160
161 ***A*/*C*$_i$ response curves**
162 The response of net photosynthesis (A) to intracellular CO_2 (C_i) was measured using a
163 portable gas exchange system (CIRAS-1, PP Systems Ltd, Ayrshire, UK). Leaves were
164 illuminated using a red-blue light source attached to the gas-exchange system, and light levels
165 were maintained at saturating photosynthetic photon flux density (PPFD) of 1000 µmol m^{-2} s^{-1}
166 with an integral LED light source (PP Systems Ltd, Ayrshire, UK) for the duration of the
167 A/C_i response curve. Measurements of A were made at ambient CO_2 concentration (C_a) of
168 400 µmol mol^{-1}, before C_a was decreased in a stepwise manner to 300, 200, 150, 100, 50
169 µmol mol^{-1} before returning to the initial value and increased to 500, 600, 700, 800, 900,
170 1000, 1100, 1200 µmol mol^{-1}. Leaf temperature and vapour pressure deficit (VPD) were

171 maintained at 22°C and 1 ± 0.2 kPa respectively. The maximum rates of Rubisco- (Vc_{max}) and
172 the maximum rate of electron transport for RuBP regeneration (J_{max}) were determined and
173 standardized to a leaf temperature of 25°C based on equations from Bernacchi et al. (2001),
174 and McMurtrie and Wang (1993) respectively.
175
176 **Photosynthetic capacity**
177 Photosynthesis as a function of PPFD (A/Q response curves) was measured using a
178 Li-Cor 6400XT portable gas exchange system (Li-Cor, Lincoln, Nebraska, USA). Cuvette
179 conditions were maintained at a leaf temperature of 22°C, relative humidity of 50-60%, and
180 ambient growth CO_2 concentration 400 µmol mol^{-1} for plants grown in ambient conditions).
181 Leaves were initially stabilized at saturating irradiance 1000 µmol m^{-2} s^{-1}, after which A and
182 g_s was measured at the following PPFD levels; 0, 50, 100, 150, 200, 250, 300, 350, 400, 500,
183 600, 800, 1000 µmol m^{-2} s^{-1}. Measurements were recorded after A reached a new steady state
184 (1-3 min) and before stomatal conductance (g_s) changed to the new light levels. A/Q analyses
185 were performed at 21% and 2% [O_2].
186
187 **PSI and PSII quantum efficiency**
188 The photochemical quantum efficiency of PSII and PSI in transgenic and WT plants
189 was measured following a dark-light induction transition using a Dual-PAM-100 instrument
190 (Walz, Effeltrich, Germany) with a DUAL-DR measuring head. Plants were dark adapted for
191 20 min before placing in the instrument. Following a dark adapted measurement plants were
192 illuminated with 220 µmol m^{-2} s^{-1} PPFD. The maximum quantum yield of PSII was
193 measured following a saturating pulse of light for 600 ms saturating pulse of light at an
194 intensity of 6200 µmol m^{-2} s^{-1}. The PSII operating efficiency was determined as described by
195 the routines above. PSI quantum efficiency was measured as an absorption change of P700

196 before and after a saturating pulse of 6200 µmol m^{-2} s^{-1} for 300 ms (which fully oxidizes
197 P700) in the presence of far-red light with a FR pre-illumination of 10s. Both measurements
198 were recorded every minute for 5 min). q_p or (F_v'/F_m'), was calculated from measurements of
199 steady state fluorescence in the light (F') and maximum fluorescence in the light (F_m') whilst
200 minimal fluorescence in the light (F_o') was calculated following the equation of Oxborough
201 and Baker (1997b). The fraction of open PSII centres (q_L) was calculated from q_p x F_o'/F
202 (Baker, 2008).
203
204 **Pigment extraction and HPLC analysis**
205 Chlorophylls and carotenoids were extracted using n,n-dimethylformamide (DMF) as
206 previously described (Inskeep and Bloom, 1985), which was subsequently shown to
207 suppressed chlorophyllide formation in Arabidopsis leaves (Hu et al., 2013). Briefly, two leaf
208 discs collected from two different leaves were immersed in DMF at 4°C for 48 hours and
209 separated by UPLC as described by Zapata et al. (2000).
210
211 **Leaf Thickness**
212 Leaves of equivalent developmental stage were collected from plants after 28 days of
213 growth. Strips were cut from the centre of the leaf, avoiding the mid-vein, preserved in 5%
214 glutaraldehyde, stored at 4°C for 24 h followed by dehydration in sequential ethanol solutions
215 of 20, 40, 80 and 100%. The samples were placed in LR white acrylic resin (Sigma-Aldrich,
216 Gillingham, UK), refrigerated for 24 h, embedded in capsules and placed at 60°C for 24 h.
217 Sections (0.5µm) were cut using a Reichert-Jung Ultracut microtome (Ametek Gmbh,
218 Munich, Germany), fixed, stained and viewed under a light microscope (Lopez-Juez et al.,
219 1998). Leaf thickness was determined by measuring leaves from two to three plants from line
220 9 and 11 compared to leaves from four wild type plants.

221

222 **Statistical Analysis**

223 All statistical analyses were done by comparing ANOVA, using Sys-stat, University of

224 Essex, UK. The differences between means were tested using the Post hoc Tukey test (SPSS,

225 Chicago).

226

227

Results

Production and selection of Rieske FeS ox transformants.

The full-length tobacco Rieske FeS coding sequence from the cyt b_6f complex was used to generate an over-expression construct B2-NtRi (Supplemental **Fig. S1**). Following floral dipping, transgenic Arabidopsis plants were selected on both kanamycin/hygromycin containing medium (Nakagawa et al., 2007) and plants expressing the integrated transgenes identified using RT-PCR (data not shown). Proteins were extracted from leaves of the T1 progeny allowing the identification of three lines with increased levels of the Rieske FeS protein (PetC) (Supplemental **Fig. S3A**). Immunoblot analysis of T3 progeny of lines 9, 10 and 11 were shown to have higher levels of the Rieske FeS protein when compared to wild type (WT) (**Fig. 1 and** Supplemental **Fig. S3B**). The over-expression of the Rieske FeS protein (hereafter referred to as Rieske FeS ox) resulted in a concomitant increase in both cyt *f* (PetA) and cyt b_6 (PetB) (**Fig. 1A**). An increase in the level of the PSI type I chlorophyll a/b-binding protein (LhcaI) and an increase in the core protein of PSI (PsaA) was also observed. Furthermore, the D1 (PsbA) and D2 (PsbD) proteins which form the reaction centre of PSII were also shown to be elevated in Rieske FeS ox lines. Finally, an increase in the ATP synthase delta subunit (AtpD) was also observed in Rieske FeS ox lines (**Fig. 1A**). In contrast, no notable differences in protein levels for either the chloroplastic FBP aldolase (FBPA), the mitochondrial glycine decarboxylase-H protein (GDC-H) or the Rubisco large subunit were observed (**Fig. 1A**). A quantitative estimate of the changes in protein levels was determined from the immunoblots of leaf extracts isolated from two to three independent plants per lines. An example is shown in **Fig. 1B**. These results showed a 2-2.5 fold increase in the Rieske Fe S protein relative to WT plants and a similar increase was also observed for cyt *f*, cyt b_6, Lhca1, D2 and PsaA (**Fig 1C**). No increase in the stromal FBPA protein was evident.

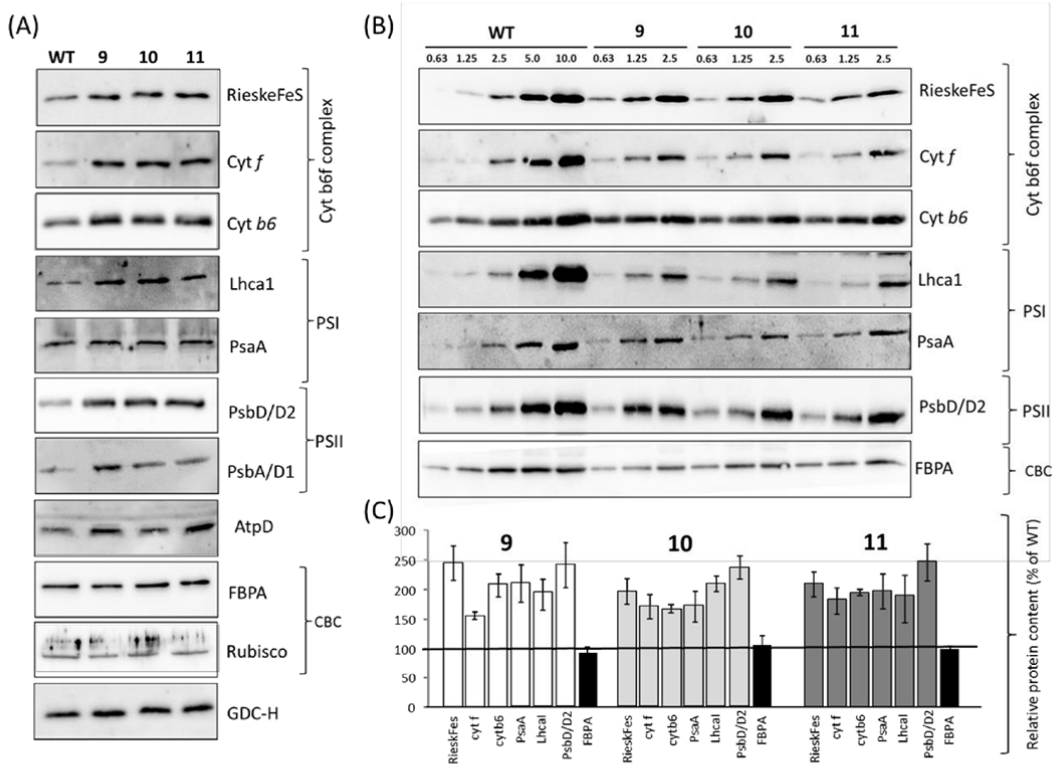

Figure 1. Immunoblot analysis of leaf proteins of wild type and Rieske FeS ox plants. Protein extracts from leaf discs taken from two leaves per plant from three independent lines (9, 10 and 11) and separated on a 12% acrylamide gel, transferred to membranes and probed with relevant antibodies. *cytochrome b6f* complex subunits, Photosystem I (PSI), Photosystem II (PSII), ATP synthase delta subunit (AtpD), Calvin-Benson cycle (CBC) proteins and the photo-respiratory GDC-H protein were probed. (A) Protein (6 μg) was loaded for all antibodies except for FBPA (3 μg) and rubisco (1 μg). (B) Proteins were loaded containing 0.63 to 10 μg of protein. (C) Protein levels were statistically analysed against WT grown plants using a one-sample t-test (* $p < 0.05$, ** $p < 0.01$) and presented as relative protein content compared to WT.

253

254 **Chlorophyll fluorescence imaging reveals increased photosynthetic efficiency in young**

255 **Rieske FeS ox seedlings.**

In order to explore the impact of increased levels of the Rieske FeS protein on photosynthesis the quantum efficiency of PSII (F_q'/F_m') was analysed using chlorophyll a fluorescence imaging (Baker, 2008; Murchie and Lawson, 2013). A small increase in F_q'/F_m' was found in the Rieske FeS ox plants at irradiances of 310 µmol m^{-2} s^{-1} and 600 µmol $m^{-2}s^{-1}$ (**Fig. 2**). Leaf area, generated from these images, was significantly larger in all Rieske FeS ox lines compared to WT (**Fig. 2C**), but no significant difference in leaf thickness was observed between the leaves of Rieske FeS lines 9 and 11 and that of the WT plants (Supplemental **Table S1**).

Photosynthetic CO_2 assimilation and electron transport rates are increased in the Rieske FeS ox plants

The impact of overexpression of the Rieske FeS protein on the rate of photosynthesis in mature plants was investigated using combined gas exchange and chlorophyll fluorescence analyses. Both the light saturated rate of CO_2 fixation (A_{sat}) and the relative light saturated rate of electron transport (rETR), were increased in the Rieske FeS ox lines compared to WT when measured at 2% [O_2] (**Fig. 3A & B; Table 1**). Additionally the light saturated rate of CO_2 assimilation at ambient [CO_2] was also increased when measured at 21% [O_2] (Supplemental **Fig. S4).** No significant difference in leaf absorbance (Abs) between the Rieske FeS ox and WT plants was found (**Table S1**). (**TABLE 1 INSERT HERE**).

In plants grown at a light level of 130 µmol m^{-2} s^{-1} no difference in the light- or CO_2 -saturated rate of CO_2 assimilation (A_{max}) was found. In contrast, in a second group of plants grown at 280 µmol $m^{-2}s^{-1}$, A_{max} was greater in the Rieske FeS ox lines 9 and 11 relative to WT (**Fig. 3C; Table 1**). Further analysis of the A/Ci curves revealed that J_{max} was significantly greater in the Rieske FeS ox plants when compared to WT **(Table 1**), but no significant difference in Vc_{max} (data not shown) was observed. (**TABLE 2 INSERT HERE**).

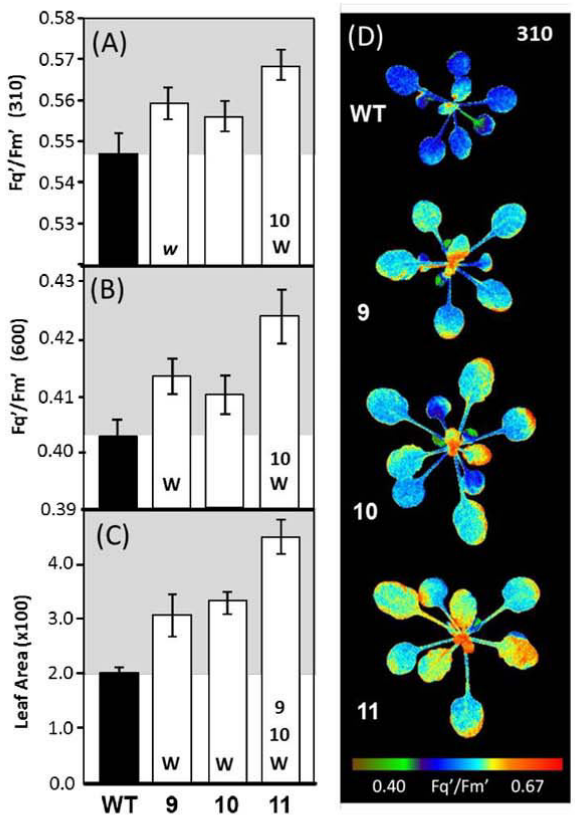

Figure 2. Determination of photosynthetic capacity and leaf area in Rieske FeS ox seedlings using chlorophyll fluorescence imaging. WT and Rieske FeS ox plants were grown in controlled environment conditions with a light intensity of 130 µmol m^{-2} s^{-1}, 8 h light/16 h dark cycle and chlorophyll fluorescence imaging used to determine $F_{q'}/F_{m'}$ (maximum PSII operating efficiency) at two light intensities 14 days after planting (DAP) (A, D) Fluorescence $F_{q'}/F_{m'}$ at 310 µmol m^{-2} s^{-1}, and (B) $F_{q'}/F_{m'}$ at 600 µmol m^{-2} s^{-1} (C) leaf area at time of analysis. The data was obtained using four to six individual plants from each line compared to WT (five plants). Significant differences ($p<0.05$) are represented as capital letters indicating differences between line. Bars represent Standard errors. Lower case italic lettering indicates lines are just below significance ($p>0.05$ - <0.1).

281

282 **The quantum efficiency of PSI and PSII was increased in the Rieske FeS ox plants**

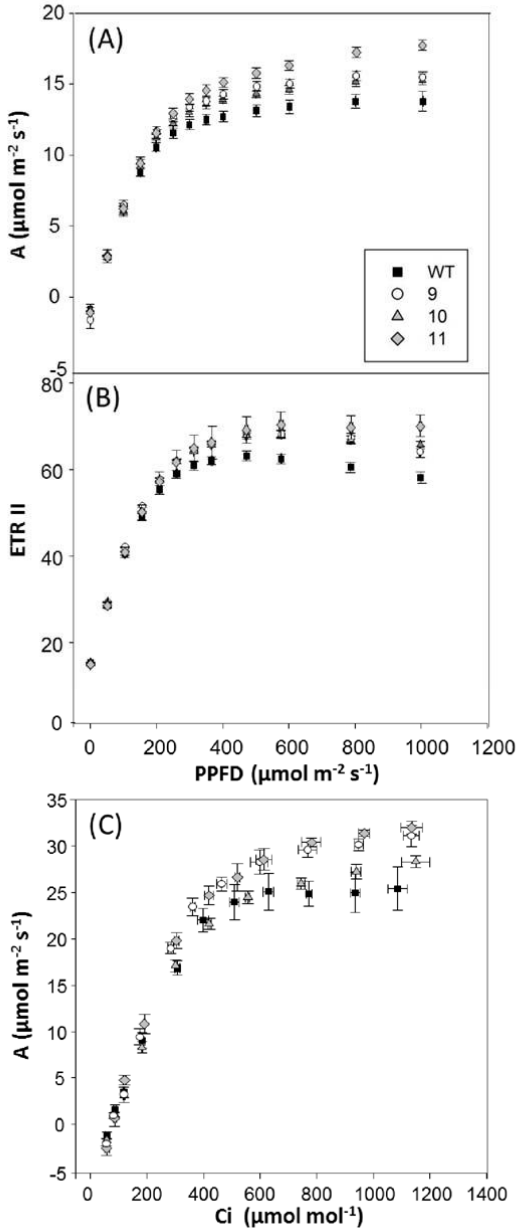

Figure 3. Photosynthetic responses of the Rieske FeS ox plants. (A) Determination of photosynthetic capacity and (B) electron transport rates in transgenic plants at 2% [O_2]. WT and transgenic plants were grown in controlled environment conditions with a light intensity 130 µmol m^{-2} s^{-1}, 8 h light/16 h dark cycle for four weeks, (C) Photosynthetic carbon fixation rate (*A*) was determined as a function of increasing CO_2 concentrations (*A*/*C*i) at saturating-light levels (1000 µmol m^{-2} s^{-1}). WT and transgenic plants were grown in controlled environment conditions at a light intensity 280 µmol m^{-2} s^{-1}, 12 h light/12 h dark cycle for four weeks. Error bars represent standard errors

283 To further explore the influence of increases in the Rieske FeS protein on PSII and
284 PSI photochemistry, dark-light induction responses were determined in WT and Rieske FeS
285 ox (lines 11 & 10) using simultaneous measurements of P700 oxidation state and PSII

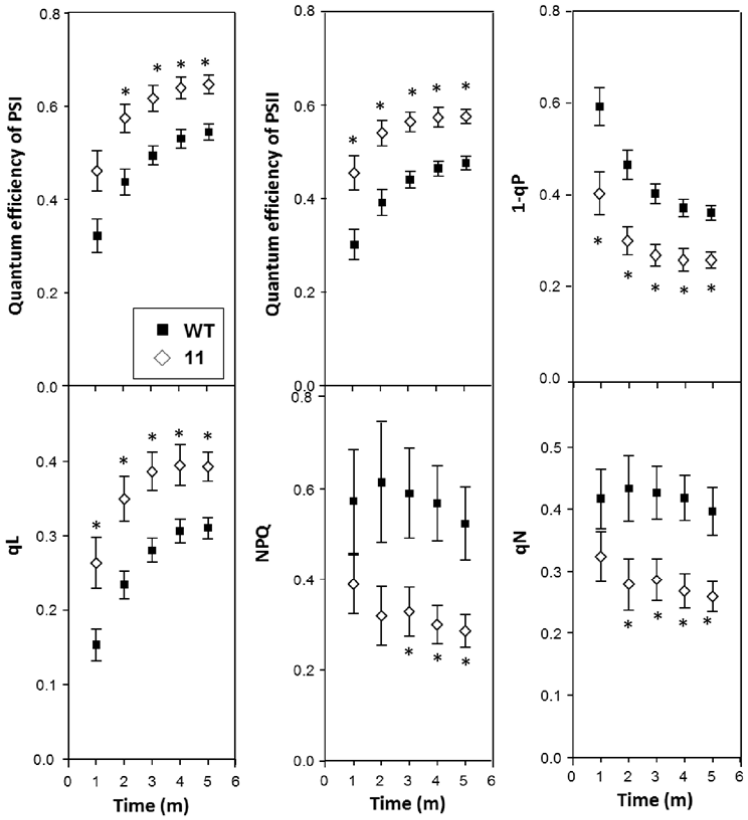

Figure 4. Determination of the efficiency of electron transport in the leaves of young Rieske Fes ox plants. WT and Rieske FeS ox plants were grown in controlled environment conditions with a light intensity of 130 μmol m^{-2} s^{-1}, 8 h light/16 h dark cycle and the redox state was determined (27 days after planting) using a Dual-PAM at a light intensity of 220 μmol m^{-2} s^{-1}. The data was obtained using four individual plants from Rieske Fes ox line 11 compared to WT (five plants). Significant differences are indicated (*p<0.05). Bars represent standard errors.

286 efficiency. These results showed that the quantum yields of both PSI and PSII were increased
287 in the Rieske FeS ox plants compared to WT and that the fraction of PSII centres that were
288 open (q_L) was also increased, whilst the level of Qa reduction (1-q_p) was lower in leaves of

27 day old plants from line 11. (**Fig .4**). NPQ levels were also shown to be lower in the Rieske FeS ox plants together with a reduction in stress induced limitation of NPQ (q_N) when compared to WT plants (**Fig. 4**). Similar results were obtained for both lines 10 and 11 when plants were analysed later in development (34 DAP) (Supplemental **Fig. S5**). The increases in the quantum yields of PSI and PSII observed here were accompanied by corresponding increase in electron transport rates (ETRI and ETRII; Supplemental **Fig. S6**).

Growth, vegetative biomass and seed yield is increased in the Rieske FeS ox plants

The leaf area of the Rieske FeS ox lines was significantly greater than WT as early as 10 days after planting in soil and by 18 days were 40-114% larger (**Fig. 5**). Destructive harvest at day 25 showed that this increase in leaf area translated to an increase in shoot biomass of between 29% - 72% determined as dry weight (**Fig. 5C**). To determine the impact of increased Rieske FeS protein on seed yield and final shoot biomass a second group of plants was grown in the same conditions as described in **Fig 6**. Interestingly, 38 days after planting (DAP) 40% of the Rieske FeS ox plants had flowered in contrast to 22% in the WT plants (**Fig. 6A**). Following seed set (52 DAP) both vegetative biomass (**Fig. 6B**) and seed yield (**Fig. 6C**) were determined and although a significant increase in biomass was observed in all of the Rieske FeS ox plants a statically significant increase in seed yield was only evident in line 11.

The pigment content was altered in the Rieske FeS ox plants.

The pigment composition of the leaves of the Rieske FeS ox and WT plants was determined. An increase in the levels of chlorophyll a and b (14-29%) was observed in the Rieske FeS ox compared to WT plants (**Fig. 7).** These increases were accompanied by an increase in the carotenoids, neoxanthin (+38%), violaxanthin (+59%), lutein (+75%) and β-

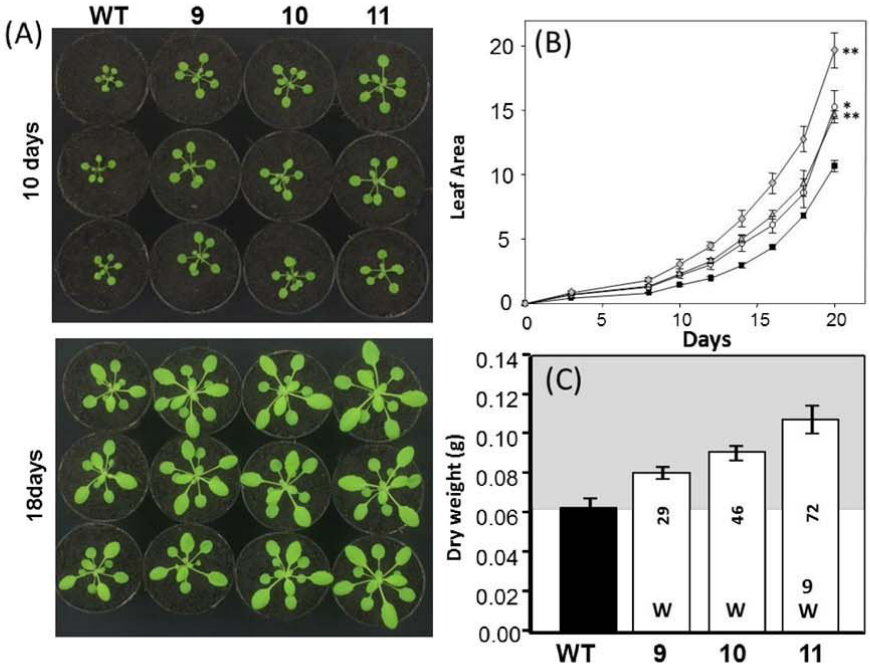

Figure 5. Growth analysis of WT and Rieske FeS ox plants. Plants were grown at 130 µmol m^{-2} s^{-1} light intensity in long days (8 h/16 h days). (A) appearance of plants at 10 and 18 days after planting (DAP). (B) Leaf area determined 20 DAP. (C) Final biomass at 25 DAP. Results are representative of six to nine plants from each line. Increase over WT (%) is indicated as numbers on histogram. Significant differences ($p<0.05$) are represented by capital letters. Significant differences * ($p<0.01$), ** ($p<0.001$), are indicated. Bars represent Standard errors.

314 carotene (+169%). No detectable change in the level of zeaxanthin was evident in the Rieske

315 FeS ox plants.

316

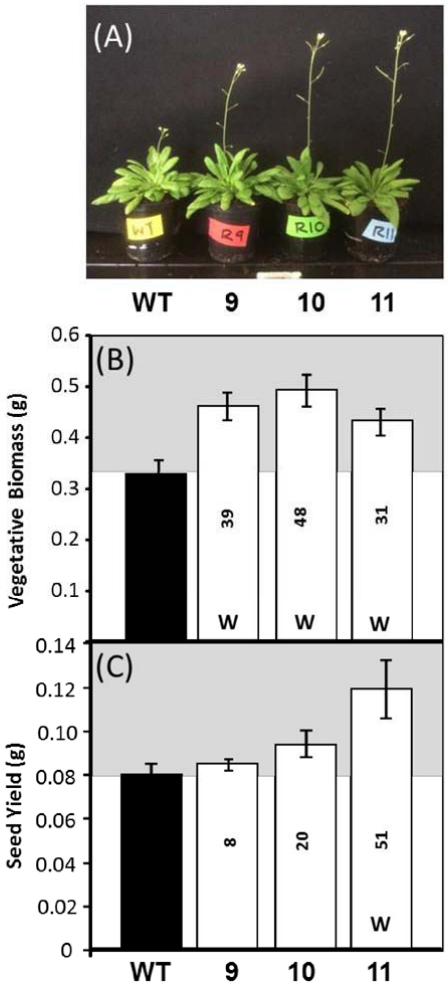

Figure 6. Seed yield and vegetative biomass of WT and Reiske FeS ox plants grown in low light. Plants were grown at 130 µmol m^{-2} s^{-1} light intensity in long days (8 h/16 h days). (A) appearance of plants at 38 DAP. (B) final biomass and (C) seed yield at harvest (52 DAP). Increase over wild type (%) is indicated by numbers on histogram. Results are representative of six to nine plants from each line. Significant differences ($p<0.05$) are represented by capital letters. Bars represent Standard errors.

317

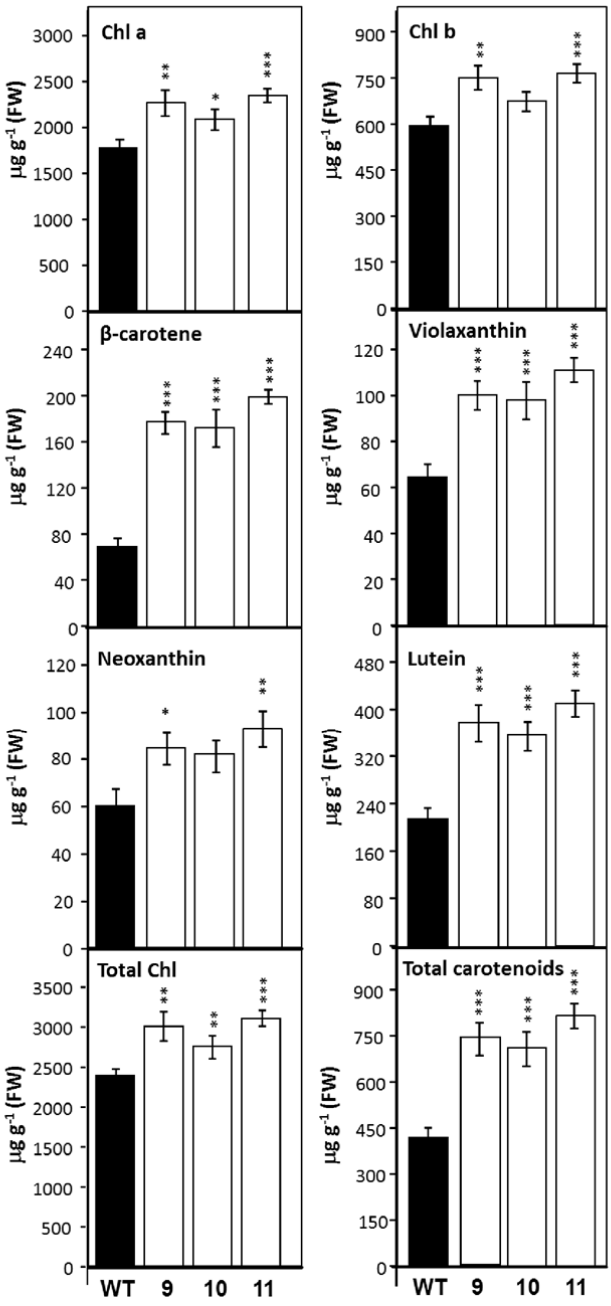

Figure 7. Pigment content in WT and Rieske FeS ox plants. Plants were grown at 130 µmol m^{-2} s^{-1} light intensity in short days (8h/16h days). Two leaf discs, collected from two different leaves, were immersed in DMF at 4°C for 48 hours and separated by UPLC. Results are represented as µg/g^{-1} fresh weight. Statistical differences are shown in bold (* p<0.1; ** p<0.05; *** p<0.001). Bars represent standard errors.

Discussion

In recent years increasing the rate of photosynthetic carbon assimilation has been identified as a target for improvement to increase yield. Evidence to support this has come from the

theory and modelling of the photosynthetic process, growth of plants in elevated CO_2 and also from transgenic manipulation (Zhu et al., 2010). It was shown previously in antisense studies that reducing the levels of the Rieske FeS protein resulted in a reduction in levels of the cyt b_6f complex, a decrease in photosynthetic electron transport and in rice a decrease in both biomass and seed yield was observed (Price et al., 1998; Yamori et al., 2016). These findings identified the cyt b_6f complex as a limiting step in electron transport and would suggest that over expression of the Rieske FeS protein may be a feasible route to increase photosynthesis and yield. In this study we show that overexpression of the Rieske FeS protein in Arabidopsis results in an increase in photosynthesis, vegetative biomass and seed yield.

Increased levels of the Rieske FeS protein increased photosynthetic electron transport, CO_2 assimilation and biomass

Using chlorophyll fluorescence imaging we have shown that that overexpression of the Rieske FeS protein resulted in an increase in photosynthesis and growth which is evident from the early stages of seedling development. These observed increases in F_q'/F_m' represent an early indication that the potential quantum yield of PSII photochemistry had been elevated in Rieske ox lines (Genty et al., 1989; Genty et al., 1992; Baker et al., 2007). This early stimulation is maintained into maturity and an increase in the light saturated rate of CO_2 assimilation and electron transport rates was evident in the Rieske FeS ox plants. Our data also showed that quantum yields of both PSII and PSI were increased and that the fraction of PSII centres available for photochemistry was increased indicated by an increase in (q_L) and a lower 1-q_p (Baker et al., 2007; Baker and Oxborough, 2004; Kramer et al., 2004). These results are consistent with what would be predicted from results obtained from the Rieske FeS antisense studies where ETR was reduced (Price. et al., 1998; Ruuska et al., 2000; Yamori et al,. 2011a). However, the impact of overexpression of the Rieske FeS protein was

346 clearly not restricted to increasing the activity of the cyt b_6/f complex but resulted in an
347 increase in electron flow through the entire electron transport chain.

348 Substantial and significant increases in the growth of the rosette area were observed in
349 the Rieske FeS ox plants in the early vegetative phase which resulted in an approximately 30-
350 70% increase in biomass yield in the different lines. Importantly seed yields in line 11, which
351 showed the biggest increases in shoot biomass were also shown to be increased relative to
352 WT.

353

354 **The Rieske FeS ox plants have increased levels of proteins in the cyt *b_6f*, PSI and PSII**
355 **complexes**

356 In keeping with our analysis of the electron transport processes in the Rieske FeS ox plants,
357 an increase in the levels of the cyt b_6 and cyt *f*, core proteins of the cyt *b_6f* complex was
358 evident. Furthermore an increase in the levels of proteins in both PSII and PS1 and the δ
359 subunit of the ATPase complex was also observed. This result was unexpected given that no
360 changes in components of PSII or PSI were observed in the Rieske FeS antisense plants.
361 Interestingly, a recent study reported increases in cyt *b_6f* proteins levels in Arabidopsis plants
362 grown under square wave light, compared to plants grown under fluctuating light, and these
363 were matched by increased levels of PSII, PSI and the δ subunit of the ATPase proteins,
364 which agrees with our study (Vialet-Chabrand et al., 2017). Furthermore, the *hcf* mutant, in
365 which the biogenesis of the cyt *b_6f* was inhibited, had a reduced accumulation of components
366 of both PSI and PSII, although these complexes remained fully functional, as inferred from
367 spectroscopic analyses, and no mechanism controlling these changes has been identified
368 (Lennartz et al., *2001*). Despite considerable efforts to gain insight into the mechanisms
369 underlying the regulation of synthesis and assembly of components of the thylakoid
370 membrane, the factors determining accumulation of these complexes are still poorly

371 understood but our results provide evidence that the Rieske FeS protein levels may play a
372 role in this regulation (Schöttler, 2015).
373
374 **Over-expression of Rieske FeS significantly modifies pigment content of leaves**
375 In parallel with the increase in components of the thylakoid membranes, plants with increased
376 Rieske FeS protein were found to have an increase in levels of both chlorophyll a and b and a
377 small increase in the chlorophyll a to b ratio from 2.96 to 3.12. The increase in chlorophyll a
378 and b suggest a greater investment in both light capture and PSII reactions centres and would
379 fit with the increase in photosynthetic electron transport capacity in the Rieske FeS ox plants.
380 In previous work, plants with reduced levels of the Rieske FeS protein had a lower
381 chlorophyll *a*/*b* ratio (Hurry et al., 1996; Price et al., 1998) which is the opposite to what was
382 observed in the Rieske FeS ox plants. In addition to increases in chlorophyll, significant
383 increases in the carotenoid pigments were also seen with β-carotene, violaxanthin (+59%),
384 lutein (+75%) and neoxanthin (+37%). β-carotene is a component of both the RC and light
385 harvesting complex (Kamiya and Shen, 2003; Ferreira et al., 2004; Loll et al., 2005; Litvin et
386 al., 2008; Janik et al., 2016) and the increase in these pigments observed in the Rieske FeS ox
387 plants is in agreement with investment in both light harvesting and increasing RC efficiency.
388
389 Lutein, neoxanthin and violaxanthin are the main xanthophyll pigment constituents of the
390 largest light-harvesting pigment-protein complex of photosystem II (LHCII) (Thayer and
391 Björkman, 1992; Ruban et al., 1994; Ruban et al., 1999; Ruban et al., 2012; Janik et al.,
392 2016). Acidification of the thylakoid lumen as a result of electron transport (and driven in
393 particular by the activities of the cytochrome b_6f complex) is accompanied by the de-
394 epoxidation of violaxanthin and an accumulation of zeaxanthin (Björkman and Demmig-
395 Adams, 1994; Muller et al., 2001; Ruban et al., 2012), as well as protonation of carboxylic

acid residues of the PsbS protein associated with PSII antennae (Li et al., 2000, 2004). Protonation of PsbS and binding of zeaxanthin increase NPQ and the thermal dissipation of excitation energy (Baker, 2008; Jahns and Holzwarth, 2012). Increases in electron transport observed in Rieske FeS ox lines might be expected to result in the acidification of the thylakoid lumen and an increase in NPQ. However, we found that the increase in the level of the Rieske FeS protein led to a small but significantly lower steady state levels of NPQ and an increase in the rate of relaxation of NPQ following illumination. The absence of an increase in NPQ in the presence of significant increases in electron transport rates suggest that the Rieske FeS ox plants also have increased rates of ATP synthesis. Although we provide no direct support for this we did observe and increase in the level of the ATP synthase delta subunit protein in the Rieske FeS ox plants. Support for this comes from the earlier work on the Rieske FeS antisense plants showing that the levels of ATP synthase were reduced and that a low transthylakoid pH gradient was evident (Price et al., 1995, 1998 Ruuska et al., 2000).

Conclusion

A number of studies have shown that increasing photosynthesis through the manipulation of CO_2 assimilation can improve growth (Miyagawa et al., 2001; Lefebvre et al., 2005; Rosenthal et al., 2011; Uematsu et al., 2012; Simkin et al., 2015, 2017), this work together with a study in which cytochrome C_6 from the red alga *Porphyra*, was expressed in Arabidopsis (Chida *et al*., 2007) provide direct evidence that there is also an opportunity to improve the efficiency of the electron transfer chain. Our results demonstrate that overexpression of the Rieske FeS protein can increase electron transport, photosynthesis and yield and provides another potential avenue to improve crop productivity and meet the food requirements for future population growth. Furthermore, overexpression of the Rieske FeS

421 protein may offer tool to investigate fundamental questions on factors controlling the
422 biogenesis of the photosynthetic complexes in the electron transport chain.
423
424 **ACKNOWLEDGMENTS**.
425 We thank James E. Fox and Philip A. Davey for help with pigment analysis and Elena A.
426 Pelech for help with Dual-PAM measurements. A.J.S was supported by BBSRC (Grant:
427 BB/J004138/1 awarded to C.A.R and T.L): A.J.S generated transgenic plants and performed
428 molecular and biochemical experiments and carried out plant phenotypic and growth
429 analysis. A.J.S and L.M performed gas exchange measurement on Arabidopsis. A.J.S and
430 L.M carried out data analysis on their respective contributions. C.R and T.L designed and
431 supervised the research. C.R, A.J.S wrote the manuscript with input from TL.
432

433 **Figure Legends**

434 **Figure 1. Immunoblot analysis of leaf proteins of wild type and Rieske FeS ox plants.**
435 Protein extracts from leaf discs taken from two leaves per plant from three independent lines
436 (9, 10 and 11) and separated on a 12% acrylamide gel, transferred to membranes and probed
437 with relevant antibodies. *cytochrome b6f* complex subunits, Photosystem I (PSI),
438 Photosystem II (PSII), ATP synthase delta subunit (AtpD), Calvin-Benson cycle (CBC)
439 proteins and the photo-respiratory GDC-H protein were probed. (A) Protein (6 µg) was
440 loaded for all antibodies except for FBPA (3 µg) and rubisco (1 µg). (B) Proteins were
441 loaded containing 0.63 to 10 µg of protein. (C) Protein levels were statistically analysed
442 against WT grown plants using a one-sample t-test (* $p < 0.05$, ** $p < 0.01$) and presented as
443 relative protein content compared to WT.
444
445 **Figure 2. Determination of photosynthetic capacity and leaf area in Rieske FeS ox**
446 **seedlings using chlorophyll fluorescence imaging.** WT and Rieske FeS ox plants were
447 grown in controlled environment conditions with a light intensity of 130 µmol m^{-2} s^{-1}, 8 h
448 light/16 h dark cycle and chlorophyll fluorescence imaging used to determine F_q'/F_m'
449 (maximum PSII operating efficiency) at two light intensities 14 days after planting (DAP) (A,
450 D) Fluorescence F_q'/F_m' at 310 µmol m^{-2} s^{-1}, and (B) F_q'/F_m' at 600 µmol m^{-2} s^{-1} (C) leaf area
451 at time of analysis. The data was obtained using four to six individual plants from each line
452 compared to WT (five plants). Significant differences ($p<0.05$) are represented as capital
453 letters indicating differences between line. Bars represent Standard errors. Lower case italic
454 lettering indicates lines are just below significance ($p>0.05$ - <0.1).
455
456 **Figure 3. Photosynthetic responses of the Rieske FeS ox plants.** (A) Determination of
457 photosynthetic capacity and (B) electron transport rates in transgenic plants at 2% [O_2]. WT
458 and transgenic plants were grown in controlled environment conditions with a light intensity
459 130 µmol m^{-2} s^{-1}, 8 h light/16 h dark cycle for four weeks, (C) Photosynthetic carbon fixation
460 rate (A) was determined as a function of increasing CO_2 concentrations (A/C_i) at saturating-
461 light levels (1000 µmol m^{-2} s^{-1}). WT and transgenic plants were grown in controlled
462 environment conditions at a light intensity 280 µmol m^{-2} s^{-1}, 12 h light/12 h dark cycle for
463 four weeks. Error bars represent standard errors.
464

Figure 4. Determination of the efficiency of electron transport in the leaves of young Rieske Fes ox plants. WT and Rieske FeS ox plants were grown in controlled environment conditions with a light intensity of 130 mmol m^{-2} s^{-1}, 8 h light/16 h dark cycle and the redox state was determined (27 days after planting) using a Dual-PAM at a light intensity of 220 µmol m^{-2} s^{-1}. The data was obtained using four individual plants from Rieske Fes ox line 11 compared to WT (five plants). Significant differences are indicated (*$p<0.05$). Bars represent standard errors.

Figure 5. Growth analysis of WT and Rieske FeS ox plants. Plants were grown at 130 µmol m^{-2} s^{-1} light intensity in long days (8 h/16 h days). (A) appearance of plants at 10 and 18 days after planting (DAP). (B) Leaf area determined 20 DAP. (C) Final biomass at 25 DAP. Results are representative of six to nine plants from each line. Increase over WT (%) is indicated as numbers on histogram. Significant differences ($p<0.05$) are represented by capital letters. Significant differences * ($p<0.01$), ** ($p<0.001$), are indicated. Bars represent standard errors.

Figure 6. Seed yield and vegetative biomass of WT and Reiske FeS ox plants. Plants were grown at 130 µmol m^{-2} s^{-1} light intensity in long days (8 h/16 h days). (A) Appearance of plants at 38 DAP. (B) final biomass and (C) seed yield at harvest (52 DAP). Increase over wild type (%) is indicated by numbers on histogram. Results are representative of six to nine plants from each line. Significant differences ($p<0.05$) are represented by capital letters. Bars represent standard errors.

Figure 7. Pigment content in WT and Rieske FeS ox plants. Plants were grown at 130 µmol m^{-2} s^{-1} light intensity in short days (8h/16 h days). Two leaf discs, collected from two different leaves, were immersed in DMF at 4°C for 48 hours and separated by UPLC. Results are represented as µg/g^{-1} fresh weight. Statistical differences are shown in bold (* $p<0.1$; ** $p<0.05$; *** $p<0.001$). Bars represent standard errors.

Table 1. Photosynthetic parameters of WT and Rieske FeS ox lines determined from light response (*AQ*) curves carried out at 2% [O_2] (see Fig. 3a and 3b). Statistical differences are shown in bold (* $p<0.1$; ** $p<0.05$; *** $p<0.01$). Standard errors are shown

Table 2. Maximum electron transport rate (J_{max}) and maximum assimilation (A_{max}) in WT and Rieske FeS ox lines derived from the A/C_i response curves shown in Fig. 3c using the equations published by von Caemmerer and Farquhar (1981). Statistical differences are shown in bold (* $p<0.1$; ** $p<0.05$;). Standard errors are shown.

Supplementary Information

Figure S1. Schematic representation of the RieskeFeS over-expression vector pGWRi used to transform Arabidopsis (Col-0). cDNA are under transcriptional control of the 35s tobacco mosaic virus promoter (*35S*), which directs constitutive high-level transcription of the transgene, and followed by the *nos* 3' terminator (*NosT*). Following floral dipping, transgenic Arabidopsis plants were selected on both kanamycin (*NPTII*) and hygromycin (*HPT*) containing medium (Nakagawa *et al.* 2007). *RB*; T-DNA right border, *LB*; T-DNA left border, *NosP*; nopaline synthase promoter.

Figure S2. Determination of photosynthetic capacity and leaf area of WT versus azygous (AZY) segregating controls using chlorophyll fluorescence imaging. WT and AZY plants were grown in controlled environment conditions with a light intensity of 130 µmol m^{-2} s^{-1}, 8 h light/16 h dark cycle for 14 days and chlorophyll fluorescence imaging used to determine F_q'/F_m' (maximum PSII operating efficiency) at a light intensity of (A) 200 µmol m^{-2} s^{-1}. (B) 600 µmol m^{-2} s^{-1} (The data was obtained using 4 individual plants from each line). (C) leaf area at time of analysis.

Figure S3. Immunoblot analysis of WT and Rieske FeS ox proteins. (A) Leaf protein extract from leaves from 27 independent T1 transformants. Protein levels were compared to PCR negative lines (AZ). Lines 9, 10 and 11 were selected for further analysis. (B) Protein gradients were loaded for two independent plants per line containing 0.63 to 10µg of protein.

Figure S4. Light Response curves of the Rieske FeS plants at 21% [O_2]. (A) Light Response Curves for each Rieske FeS lines compared to wild type (WT). The data was obtained using four individual Rieske FeS ox and WT plants. Standard errors are shown. (B)

530 the photosynthetic parameters of WT and Rieske FeS ox lines determined from light response
531 (*AQ*) curves.
532
533 **Figure S5. Determination of the efficiency of electron transport in the leaves of mature**
534 **Rieske Fes ox plants (lines 10 & 11, 34 days after planting).** WT and Rieske FeS ox plants
535 were grown in controlled environment conditions with a light intensity of 130 µmol m^{-2} s^{-1}, 8
536 h light/16 h dark cycle and the redox state was determined using a Dual-PAM at a light
537 intensity of 220 µmol m^{-2} s^{-1} . The data was obtained using four individual plants from Rieske
538 Fes ox line (A) 10 and (B) 11 compared to WT (five plants). Significant differences are
539 indicated (*$p<0.05$). Bars represent Standard errors.
540
541 **Figure S6. Determination of the efficiency of electron transport in the leaves of (A)**
542 **young (line 11, (27 days after planting)) and (B) mature Rieske Fes ox plants (lines 10 &**
543 **11, (34 days after planting respectively)).** WT and Rieske FeS ox plants were grown in
544 controlled environment conditions with a light intensity of 130 µmol m^{-2} s^{-1}, 8 h light/16 h
545 dark cycle and the redox state was determined using a Dual-PAM at a light intensity of 220
546 µmol m^{-2} s^{-1} . The data was obtained using four individual plants from Rieske Fes ox line
547 Significant differences are indicated (*$p<0.05$). Bars represent Standard errors.
548
549 **Table S1. Physiological parameters of Rieske FeS ox plants compared to WT.** The data
550 was obtained using four individual Rieske FeS ox and WT plants. Standard errors are shown.
551 WT and Rieske FeS ox plants were grown in controlled environment conditions with a light
552 intensity of 130 µmol m^{-2} s^{-1}, 8 h light/16 h dark cycle
553
554

Table 1. the photosynthetic parameters of WT and Rieske FeS ox lines determined from light response curves (*A*Q) curves carried out at 2% [O_2] (see Fig. 3a and 3b). Statistical differences are shown in bold (* p<0.1; ** p<0.05; *** p<0.01). Standard errors are shown

	***A/Q* 2% [O_2]**				
Name	Light (μmol m^{-2} s^{-1})	F_q'/F_m'	ETRII (μmol e^- m^{-2} s^{-1})	q_P	A_{sat} (μmol m^{-2} s^{-1})
WT	400	0.343 ± 0.013	62.3 ± 0.96	0.58 ± 0.02	
	1000	0.124 ± 0.002	54.4 ± 0.91	0.23 ± 0.01	14.7 ± 0.35
9	400	**0.380 ± 0.004 ****	**66.5 ± 0.46 ****	**0.64 ± 0.00 ****	
	1000	**0.151 ± 0.002 *****	**65.9 ± 0.79 *****	**0.28 ± 0.00 ****	**16.5 ± 0.13 ****
10	400	0.369 +/-0.009	**65.9 ± 0.68 ****	0.62 ± 0.01	
	1000	**0.147 ± 0.003 *****	**64.3 ± 1.24 *****	**0.27 ± 0.00 ***	**17.7 ± 0.87 *****
11	400	0.370 ± 0.018	66.4 ± 3.73	0.63 ± 0.02	
	1000	**0.156 ± 0.006 *****	**70.3 ± 2.47 *****	**0.29 ± 0.00 *****	**18.4 ± 0.44 *****

Table 2. the maximum electron transport rate (J_{max}) and maximum assimilation (A_{max}) in WT and Rieske FeS ox lines derived from the *A*/Ci response curves shown in Fig. 3c using the equations published by von Caemmerer and Farquhar (1981). Statistical differences are shown in bold (* p<0.1; ** p<0.05;). Standard errors are shown.

	***A* /Ci**	
Name	J_{max} (μmol m^{-2} s^{-1})	A_{max} (μmol m^{-2} s^{-1})
WT	181 ± 11.6	24.4 ± 2.31
9	**210 ± 10.2 ***	**31.1 ± 1.14 ****
10	194 ± 8.9	28.3 ± 0.67
11	**216 ± 11.9 ****	**31.9 ± 0.68 ****

Parsed Citations

Anderson JM (1992) Cytochrome b6f complex: dynamic molecular organization, function and acclimation. Photosynth Res 34: 341-357
Pubmed: Author and Title
CrossRef: Author and Title
Google Scholar: Author Only Title Only Author and Title

Anderson JM, Price GD, Chow WS, Hope AB. Badger MR (1997) Reduced levels of cytochrome bf complex in transgenic tobacco leads to marked photochemical reduction of the plastoquinone pool, without significant change in acclimation to irradiance. Photosynth Res 53: 215-227
Pubmed: Author and Title
CrossRef: Author and Title
Google Scholar: Author Only Title Only Author and Title

Baker NR (2008) Chlorophyll fluorescence: a probe of photosynthesis in vivo. (2008). Annu Rev Plant Biol 59: 89-113
Pubmed: Author and Title
CrossRef: Author and Title
Google Scholar: Author Only Title Only Author and Title

Baker NR, Oxborough K, Lawson T, Morison JI (2001) High resolution imaging of photosynthetic activities of tissues, cells and chloroplasts in leaves. . J Exp Bot 52: 615-621
Pubmed: Author and Title
CrossRef: Author and Title
Google Scholar: Author Only Title Only Author and Title

Baker NR, Rosenqvist E (2004) Applications of chlorophyll fluorescence can improve crop production strategies: an examination of future possibilities. J Exp Bot 55: 1607-1621
Pubmed: Author and Title
CrossRef: Author and Title
Google Scholar: Author Only Title Only Author and Title

Baniulis D, Yamashita E, Whitelegge JP, Zatsman AI, Hendrich MP, Hasan SS, Ryan CM, Cramer WA (2009) Structure-function, stability, and chemical modification of the cyanobacterial cytochrome b6f complex from Nostoc sp. PCC 7120. J Biol Chem 284: 9861-9869
Pubmed: Author and Title
CrossRef: Author and Title
Google Scholar: Author Only Title Only Author and Title

Barbagallo RP, Oxborough K, Pallett KE, Baker N.R (2003) Rapid, non-invasive screening for perturbations of metabolism and plant growth using chlorophyll fluorescence imaging. Plant Physiol 132: 485-493
Pubmed: Author and Title
CrossRef: Author and Title
Google Scholar: Author Only Title Only Author and Title

Barkan A, Miles D, Taylor WC (1986) Chloroplast gene expression in nuclear photosynthetic mutants of maize. EMBO J. 5: 1421-1427
Pubmed: Author and Title
CrossRef: Author and Title
Google Scholar: Author Only Title Only Author and Title

Bernacchi CJ, Singsaas EL, Pimentel C, Portis Jr AR, Long SP (2001) Improved temperature response functions for models of Rubisco-limited photosynthesis. Plant, Cell Environ 24: 253-260
Pubmed: Author and Title
CrossRef: Author and Title
Google Scholar: Author Only Title Only Author and Title

Björkman O, Demmig-Adams B (1994) Regulation of photosynthetic light energy capture, conversion, and dissipation in leaves of higher plants. 01 E-D Schulze, MM Caldwell, eds, Ecophysiology of Photosynthesis. Springer-Verlag, Berlin, pp 1747
Pubmed: Author and Title
CrossRef: Author and Title
Google Scholar: Author Only Title Only Author and Title

Bruce BD, Malkin R. (1991) Biosynthesis of the chloroplast cytochrome b6f complex: studies in a photosynthetic mutant of Lemna. Plant Cell 3: 203-212
Pubmed: Author and Title
CrossRef: Author and Title
Google Scholar: Author Only Title Only Author and Title

Clough SJ, Bent AF (1998) Floral dip: a simplified method for Agrobacterium-mediated transformation of Arabidopsis thaliana. Plant J 16: 735-743
Pubmed: Author and Title
CrossRef: Author and Title
Google Scholar: Author Only Title Only Author and Title

Cramer WA, Zhang H (2006) Consequences of the structure of the cytochrome b6f complex for its charge transfer pathways. Biochim Biophys Acta 1757: 339-345
Pubmed: Author and Title
CrossRef: Author and Title

Google Scholar: Author Only Title Only Author and Title

Cramer WA, Zhang H, Yan J, Kurisu G, Smith JL (2006) Transmembrane traffic in the cytochrome b6f complex. Annu Rev Biochem 75: 769-790

Pubmed: Author and Title
CrossRef: Author and Title
Google Scholar: Author Only Title Only Author and Title

Chida H, Nakazawa A, Akazaki H, Hirano T, Suruga K, Ogawa M, ..., Oku T (2007). Expression of the Algal Cytochrome c6 Gene in Arabidopsis Enhances Photosynthesis and Growth. Plant Cell Physiol 48: 948-957

Pubmed: Author and Title
CrossRef: Author and Title
Google Scholar: Author Only Title Only Author and Title

Driever SM, Simkin AJ, Alotaibi S, Fisk SJ, Madgwick PJ, Sparks CA, Jones HD, Lawson T, Parry MAJ, Raines CA (2017). Increased SBPase activity improves photosynthesis and grain yield in wheat grown in greenhouse conditions. Phil. Trans. R. Soc. B. (in press)

Pubmed: Author and Title
CrossRef: Author and Title
Google Scholar: Author Only Title Only Author and Title

Ferreira KN, Iverson TM, Maghlaoui K, Barber J, Iwata S (2004) Architecture of the photosynthetic oxygen-evolving center, Science 303: 1831-1838

Pubmed: Author and Title
CrossRef: Author and Title
Google Scholar: Author Only Title Only Author and Title

Fischer RA, Edmeades GO (2010) Breeding and crop yield progress. Crop Science 50: S85-S98

Pubmed: Author and Title
CrossRef: Author and Title
Google Scholar: Author Only Title Only Author and Title

Gupta R, Mould RM, He Z, Luan S (2002) A chloroplast FKBP interacts with and affects the accumulation of Rieske subunit of cytochrome bf complex. Proc Natl Acad Sci 99: 15806-15811

Pubmed: Author and Title
CrossRef: Author and Title
Google Scholar: Author Only Title Only Author and Title

Hager M, Biehler K, Illerhaus J, Ruf S, Bock R (1999) Targeted inactivation of the smallest plastid genome-encoded open reading frame reveals a novel and essential subunit of the cytochrome b(6)f complex. EMBO J 18: 5834-5842

Pubmed: Author and Title
CrossRef: Author and Title
Google Scholar: Author Only Title Only Author and Title

Harrison EP, Willingham NM, Lloyd JC, Raines CA. (1998) Reduced sedoheptulose-1,7-bisphosphatase levels in transgenic tobacco lead to decreased photosynthetic capacity and altered carbohydrate accumulation. Planta 204: 27-36

Pubmed: Author and Title
CrossRef: Author and Title
Google Scholar: Author Only Title Only Author and Title

Hojka M, Thiele W, Toth SZ, Lein W, Bock R, Schöttler MA (2014) Inducible repression of nuclear-encoded subunits of the cytochrome b6f complex in tobacco reveals an extraordinarily long lifetime of the complex. Plant Physiol 165: 1632-1646

Pubmed: Author and Title
CrossRef: Author and Title
Google Scholar: Author Only Title Only Author and Title

Hu X, Tanaka A, Tanaka R (2013) Simple extraction methods that prevent the artifactual conversion of chlorophyll to chlorophyllide during pigment isolation from leaf samples. Plant Methods 9: 19

Pubmed: Author and Title
CrossRef: Author and Title
Google Scholar: Author Only Title Only Author and Title

Hurry V, Anderson JM, Badger MR, Price GD (1996) Reduced levels of cytochrome b 6/f in transgenic tobacco increases the excitation pressure on Photosystem II without increasing sensitivity to photoinhibition in vivo. Photosyn Res 50: 159-169

Pubmed: Author and Title
CrossRef: Author and Title
Google Scholar: Author Only Title Only Author and Title

Ingelsson B, Shapiguzov A, Kieselbach T, Vener AV (2009) Peptidyl-Prolyl Isomerase Activity in Chloroplast Thylakoid Lumen is a Dispensable Function of Immunophilins in Arabidopsis thaliana. Plant Cell Physiol 50: 1801-1814

Pubmed: Author and Title
CrossRef: Author and Title
Google Scholar: Author Only Title Only Author and Title

Inskeep WP, Bloom PR (1985) Extinction coefficients of chlorophyll a and b in n,n-dimethylformamide and 80% acetone. Plant Physiol 77: 483-485

Pubmed: Author and Title
CrossRef: Author and Title
Google Scholar: Author Only Title Only Author and Title

Jahns P, Holzwarth AR (2012) The role of the xanthophyll cycle and of lutein in photoprotection of photosystem II. Biochim Biophys

Acta 1817: 182-193
Pubmed: Author and Title
CrossRef: Author and Title
Google Scholar: Author Only Title Only Author and Title

Janik E, Bednarska J, Zubik M, Sowinski K, Luchowski R, Grudzinski W, Matosiuk D, Gruszecki WI (2016) The xanthophyll cycle pigments, violaxanthin and zeaxanthin, modulate molecular organization of the photosynthetic antenna complex LHCII. Arch Biochem Biophys 592: 1-9
Pubmed: Author and Title
CrossRef: Author and Title
Google Scholar: Author Only Title Only Author and Title

Kamiya N, Shen JR (2003) Crystal structure of oxygen-evolving photosystem II from Thermosynechococcus vulcanus at 3.7-A° resolution, Proc Natl Acad Sci 100: 98-103
Pubmed: Author and Title
CrossRef: Author and Title
Google Scholar: Author Only Title Only Author and Title

Kana R, Kotabová E, Kopecná J, Trsková E, Belgio E, Sobotka R, Ruban AV (2016) Violaxanthin inhibits nonphotochemical quenching in light-harvesting antenna of Chromera velia. FEBS Letters 590: 1076-1085.
Pubmed: Author and Title
CrossRef: Author and Title
Google Scholar: Author Only Title Only Author and Title

Kirchhoff H, Horstmann S, Weis E (2000) Control of photosynthetic elec tron transport by PQ diffusion microdomains in thylakoids of higher plants. Biochim Biophys Acta 1459: 148-168
Pubmed: Author and Title
CrossRef: Author and Title
Google Scholar: Author Only Title Only Author and Title

Knight JS, Duckett CM, Sullivan JA, Walker AR, Gray JC (2002) Tissue-specific, light-regulated and plastid-regulated expression of the single-copy nuclear gene encoding the chloroplast Rieske FeS protein of Arabidopsis thaliana. Plant Cell Physiol 43: 522-531
Pubmed: Author and Title
CrossRef: Author and Title
Google Scholar: Author Only Title Only Author and Title

Kuras R, Wollman FA (1994) The assembly of cytochrome b6/f complexes: an approach using genetic transformation of the green alga Chlamydomonas reinhardtii. EMBO J 13: 1019-1027
Pubmed: Author and Title
CrossRef: Author and Title
Google Scholar: Author Only Title Only Author and Title

Lefebvre S, Lawson T, Zakhleniuk OV, Lloyd JC, and Raines CA (2005) Increased sedoheptulose-1,7-bisphosphatase activity in transgenic tobacco plants stimulates photosynthesis and growth from an early stage in development. Plant Physiol 138, 451-460
Pubmed: Author and Title
CrossRef: Author and Title
Google Scholar: Author Only Title Only Author and Title

Lennartz K, Henning P, Seidler A, Westhoff P, Bechtold N, Meierhoff K (2001) HCF164 Encodes a Thioredoxin-Like Protein Involved in the Biogenesis of the Cytochrome b6f Complex in Arabidopsis. Plant Cell 13: 2539-2551.
Pubmed: Author and Title
CrossRef: Author and Title
Google Scholar: Author Only Title Only Author and Title

Li XP, Bjorkman O, Shih C, Grossman AR, Rosenqvist M, Jansson S, Niyogi KK (2000) A pigment-binding protein essential for regulation of photosynthetic light harvesting. Nature 403: 391-395
Pubmed: Author and Title
CrossRef: Author and Title
Google Scholar: Author Only Title Only Author and Title

Li XP, Gilmore AM, Caffarri S, Bassi R, Golan T, Kramer D, Niyogi KK (2004) Regulation of photosynthetic light harvesting involves intrathylakoid lumen pH sensing by the PsbS protein. J Bio Chem 279: 22866-22874
Pubmed: Author and Title
CrossRef: Author and Title
Google Scholar: Author Only Title Only Author and Title

Litvin R, Bina D, Vacha F (2008) Room temperature photooxidation of beta-carotene and peripheral chlorophyll in photosystem II reaction centre. Photosynth Res 98: 179-187
Pubmed: Author and Title
CrossRef: Author and Title
Google Scholar: Author Only Title Only Author and Title

Loll B, Kern J, Saenger W, Zouni A, Biesiadka J (2005) Towards complete cofactor arrangement in the 3.0 A ° resolution structure of photosystem II. Nature 438: 1040-1044
Pubmed: Author and Title
CrossRef: Author and Title
Google Scholar: Author Only Title Only Author and Title

Long SP, Marshall-Colon A, Zhu ZG (2015) Meeting the Global Food Demand of the Future by Engineering Crop Photosynthesis and Yield Potential. Cell 161: 56-66

Pubmed: Author and Title
CrossRef: Author and Title
Google Scholar: Author Only Title Only Author and Title

López-Juez E, Jarvis RP, Takeuchi A, Page AM, Chory J (1998) New Arabidopsis cue mutants suggest a close connection between plastid-and phytochrome regulation of nuclear gene expression. Plant Physiol 118: 803-815
Pubmed: Author and Title
CrossRef: Author and Title
Google Scholar: Author Only Title Only Author and Title

McMurtrie RE, Wang YP (1993) Mathmatical models of the photosynthetic response of tree stands to rising CO2 concentrations and temperature Plant, Cell Environ 16: 1-13
Pubmed: Author and Title
CrossRef: Author and Title
Google Scholar: Author Only Title Only Author and Title

Metz JG, Miles D, Rutherford AW (1983) Characterization of nuclear mutants that lack the cytochrome f/b-563 complex. Plant Physiol 73: 452-459
Pubmed: Author and Title
CrossRef: Author and Title
Google Scholar: Author Only Title Only Author and Title

Miles D (1982) The use of mutations to probe photosynthesis in higher plants. In: Edelman E, Hallick RB and Chua N-H (eds). Methods in Chloroplast Molecular Biology, pp 75-107. Elsevier Biomedical Press, Amsterdam.
Pubmed: Author and Title
CrossRef: Author and Title
Google Scholar: Author Only Title Only Author and Title

Miyagawa Y, Tamoi M, Shigeoka S (2001) Over-expression of a cyanobacterial fructose-1,6-sedoheptulose-1,7-bisphosphatase in tobacco enhances photosynthesis and growth. Nature Biotech 19: 965-969
Pubmed: Author and Title
CrossRef: Author and Title
Google Scholar: Author Only Title Only Author and Title

Monde RA, Zito F, Olive J, Wollman FA, Stern DB (2000) Posttranscriptional defects in tobacco chloroplast mutants lacking the cytochrome b6/f complex. Plant J 21: 61-72
Pubmed: Author and Title
CrossRef: Author and Title
Google Scholar: Author Only Title Only Author and Title

Müller P, Li XP, Niyogi KK (2001) Non-Photochemical Quenching. A Response to Excess Light Energy. Plant Physiol 125: 1558-1566
Pubmed: Author and Title
CrossRef: Author and Title
Google Scholar: Author Only Title Only Author and Title

Murchie EH, Lawson T (2013) Chlorophyll fluorescence analysis: guide to good practice and understanding some new applications. J Exp Bot 64: 3983-3998
Pubmed: Author and Title
CrossRef: Author and Title
Google Scholar: Author Only Title Only Author and Title

Nakagawa T, Kurose T, Hino T, Tanaka K, Kawamukai M, Niwa Y, ..., Kimura T (2007) Development of series of gateway binary vectors, pGWBs, for realizing efficient construction of fusion genes for plant transformation. J Biosci Bioeng 104: 34-41
Pubmed: Author and Title
CrossRef: Author and Title
Google Scholar: Author Only Title Only Author and Title

Oxborough K, Baker NR (1997a) An instrument capable of imaging chlorophyll a Fluorescence from intact leaves at very low irradiance and at cellular and subcellular levels. Plant, Cell Environ 20: 1473-1483
Pubmed: Author and Title
CrossRef: Author and Title
Google Scholar: Author Only Title Only Author and Title

Oxborough K, Baker NR (1997b). Resolving chlorophyll a fluorescence images of photosynthetic efficiency into photochemical and nonphotochemical components -calculation of qP and Fv/Fm without measuring Fo. Photosynth Res 54: 135-142
Pubmed: Author and Title
CrossRef: Author and Title
Google Scholar: Author Only Title Only Author and Title

Price GD, von Caemmerer S, Evans JR, Siebke K, Anderson JM, Badger MR (1998) Photosynthesis is strongly reduced by antisense suppression of chloroplastic cytochrome bf complex in transgenic tobacco. Aust J Plant Physiol 25: 445-452
Pubmed: Author and Title
CrossRef: Author and Title
Google Scholar: Author Only Title Only Author and Title

Price GD, Yu JW, von Caemmerer S, Evans JR, Chow WS, Anderson JM, Hurry V, Badger MR (1995) Chloroplast cytochromeb6/f and ATP synthase complexes in tobacco: transformation with antisense RNA against nuclear-encoded transcripts for the Rieske FeS and ATP polypeptides. Aust J Plant Physiol 22: 285-297
Pubmed: Author and Title
CrossRef: Author and Title
Google Scholar: Author Only Title Only Author and Title

Raines CA (2011) Increasing photosynthetic carbon assimilation in C3 plants to improve crop yield: current and future strategies. Plant Physiol 155: 36-42
Pubmed: Author and Title
CrossRef: Author and Title
Google Scholar: Author Only Title Only Author and Title

Raines CA (2006) Transgenic approaches to manipulate the environmental responses of the C3 carbon fixation cycle. Plant, Cell Environ 29:331-339
Pubmed: Author and Title
CrossRef: Author and Title
Google Scholar: Author Only Title Only Author and Title

Ray DK, Ramankutty N, Mueller ND, West PC, Foley JA (2012) Recent patterns of crop yield growth and stagnation. Nature Comm 3: 1293
Pubmed: Author and Title
CrossRef: Author and Title
Google Scholar: Author Only Title Only Author and Title

Rosenthal DM, Locke AM, Khozaei M, Raines CA, Long SP, Ort DR (2011) Over-expressing the C3 photosynthesis cycle enzyme Sedoheptulose-1-7 bisphosphatase improves photosynthetic carbon gain and yield under fully open air CO2 fumigation (FACE) BMC Plant Biology 11: 123
Pubmed: Author and Title
CrossRef: Author and Title
Google Scholar: Author Only Title Only Author and Title

Ruban AV, Young A, Horton P (1994) Modulation of chlorophyll fluorescence quenching in isolated light harvesting complex of photosystem-II. Biochim Biophys Acta 1186: 123-127
Pubmed: Author and Title
CrossRef: Author and Title
Google Scholar: Author Only Title Only Author and Title

Ruban AV, Young AJ, Horton P (1996) Dynamic properties of the minor chlorophyll a/b binding proteins of photosystem II, an in vitro model for photoprotective energy dissipation in the photosynthetic membrane of green plants. Biochem 35: 674-678
Pubmed: Author and Title
CrossRef: Author and Title
Google Scholar: Author Only Title Only Author and Title

Ruban AV, Lee PJ, Wentworth M, Young AJ, Horton P (1999) Determination of the stoichiometry and strength of binding of xanthophylls to the photosystem II light harvesting complexes. J Biol Chem 274: 10458-10465
Pubmed: Author and Title
CrossRef: Author and Title
Google Scholar: Author Only Title Only Author and Title

Ruban AV (2012) The photosynthetic membrane: molecular mechanisms and biophysics of light harvesting. Oxford: Wiley-Blackwell.
Pubmed: Author and Title
CrossRef: Author and Title
Google Scholar: Author Only Title Only Author and Title

Ruuska SA, Andrews TJ, Badger MR, Price GD, von Caemmerer S (2000) The role of chloroplast electron transport and metabolites in modulating rubisco activity in tobacco. Insights from transgenic plants with reduced amounts of cytochrome b/f complex or glyceraldehyde 3-phosphate dehydrogenase. Plant Physiol 122: 491-504
Pubmed: Author and Title
CrossRef: Author and Title
Google Scholar: Author Only Title Only Author and Title

Schöttler MA, Flügel C, Thiele W, Bock R (2007) Knock-out of the plastid-encoded PetL subunit results in reduced stability and accelerated leaf age-dependent loss of the cytochrome b6f complex. J Biol Chem 282: 976-985
Pubmed: Author and Title
CrossRef: Author and Title
Google Scholar: Author Only Title Only Author and Title

Schöttler MA, Tóth SZ, Boulouis A, Kahlau S (2015) Photosynthetic complex stoichiometry dynamics in higher plants: biogenesis, function, and turnover of ATP synthase and the cytochrome b6f complex. J Exp Bot 66: 2373-2400
Pubmed: Author and Title
CrossRef: Author and Title
Google Scholar: Author Only Title Only Author and Title

Schwenkert S, Legen J, Takami T, Shikanai T, Herrmann RG, Meurer J (2007) Role of the low-molecular-weight subunits PetG, PetL, and PetN in the assembly, stability and dimerization of the cytochrome b6f complex in tobacco. Plant Physiol 144: 1924-1935
Pubmed: Author and Title
CrossRef: Author and Title
Google Scholar: Author Only Title Only Author and Title

Simkin AJ, McAusland L, Headland LR, Lawson T, Raines CA (2015) Multigene manipulation of photosynthetic carbon assimilation increases CO2 fixation and biomass yield in tobacco. J Exp Bot 66: 4075-4090
Pubmed: Author and Title
CrossRef: Author and Title
Google Scholar: Author Only Title Only Author and Title

Simkin AJ, Lopez-Calcagno PE, Davey PA, Headland LR, Lawson T, Timm S, Bauwe H, Raines CA (2017) Simultaneous stimulation of sedoheptulose 1,7-bisphosphatase, fructose 1,6-bisphophate aldolase and the photorespiratory glycine decarboxylase H-protein increases CO2 assimilation, vegetative biomass and seed yield in Arabidopsis. Plant Biotechnol J. doi: 10.1111/pbi.12676
Pubmed: Author and Title
CrossRef: Author and Title
Google Scholar: Author Only Title Only Author and Title

Thayer SS, Björkman O (1992) Carotenoid distribution and de-epoxidation in thylakoid pigment-protein complexes from cotton leaves and bundle sheath cells of maize. Photosyn Res 33: 213-226
Pubmed: Author and Title
CrossRef: Author and Title
Google Scholar: Author Only Title Only Author and Title

Uematsu K, Suzuki N, Iwamae T, Inui M, Yukawa H (2012) Increased fructose 1,6-bisphosphate aldolase in plastids enhances growth and photosynthesis of tobacco plants. J Exp Bot 63: 3001-3009
Pubmed: Author and Title
CrossRef: Author and Title
Google Scholar: Author Only Title Only Author and Title

Vialet-Chabrand S, Matthews JSA, Simkin AJ, Raines CA, Lawson T (2017) Importance of fluctuations in light on plant photosynthetic acclimation. Plant Physiol doi: 10.1104/pp.16.01767
Pubmed: Author and Title
CrossRef: Author and Title
Google Scholar: Author Only Title Only Author and Title

von Caemmerer S, Farquhar G.D (1981) Some relationships between the biochemistry of photosynthesis and the gas exchange of leaves. Planta 153: 376-387
Pubmed: Author and Title
CrossRef: Author and Title
Google Scholar: Author Only Title Only Author and Title

von Caemmerer S, Furbank RT (2016) Strategies for improving C4 photosynthesis. Curr Opin in Plant Biol 31: 125-134
Pubmed: Author and Title
CrossRef: Author and Title
Google Scholar: Author Only Title Only Author and Title

Willey DL, Gray JC (1988) Synthesis and assembly of the cytochrome b-f complex in higher plants. Photosynth Res 17: 125-144
Pubmed: Author and Title
CrossRef: Author and Title
Google Scholar: Author Only Title Only Author and Title

Yamori W, Takahashi S, Makino A, Price G.D, Badger MR, von Caemmerer S (2011a) The roles of ATP synthase and the cytochrome b6/f complexes in limiting chloroplast electron transport and determining photosynthetic capacity. Plant Physiol 155: 956-962
Pubmed: Author and Title
CrossRef: Author and Title
Google Scholar: Author Only Title Only Author and Title

Yamori W, Sakata N, Suzuki Y, Shikanai T, Makino A (2011b) Cyclic electron flow around photosystem I via chloroplast NAD(P)H dehydrogenase (NDH) complex performs a significant physiological role during photosynthesis and plant growth at low temperature in rice. Plant J 68: 966-976
Pubmed: Author and Title
CrossRef: Author and Title
Google Scholar: Author Only Title Only Author and Title

Yamori W, Kondo E, Sugiura D, Terashima I, Suzuki Y, Makino A (2016) Enhanced leaf photosynthesis as a target to increase grain yield: insights from transgenic rice lines with variable Rieske FeS protein content in the cytochrome b6/f complex. Plant, Cell Environ 39: 80-87
Pubmed: Author and Title
CrossRef: Author and Title
Google Scholar: Author Only Title Only Author and Title

Zhu XG, Long SP, Ort DR (2010) Improving photosynthetic efficiency for greater yield. Annu Rev Plant Biol 61, 235-226.
Pubmed: Author and Title
CrossRef: Author and Title
Google Scholar: Author Only Title Only Author and Title

Zapata M, Rodríguez F, Garrido JL (2000) Separation of chlorophylls and carotenoids from marine phytoplankton, a new HPLC method using a reversed phase C8 column and phridine-containing mobile phases. Mar Ecol Prog Ser 195, 29-45.
Pubmed: Author and Title
CrossRef: Author and Title
Google Scholar: Author Only Title Only Author and Title

Figure S1. Schematic representation of the RieskeFeS over-expression vector pGWRi used to transform Arabidopsis (Col-0). cDNA are under transcriptional control of the 35s tobacco mosaic virus promoter (*35S*), which directs constitutive high-level transcription of the transgene, and followed by the *nos* 3' terminator (*NosT*). Following floral dipping, transgenic Arabidopsis plants were selected on both kanamycin (*NPTII*) and hygromycin (*HPT*) containing medium (Nakagawa *et al.* 2007). *RB*; T-DNA right border, *LB*; T-DNA left border, *NosP*; nopaline synthase promoter,.

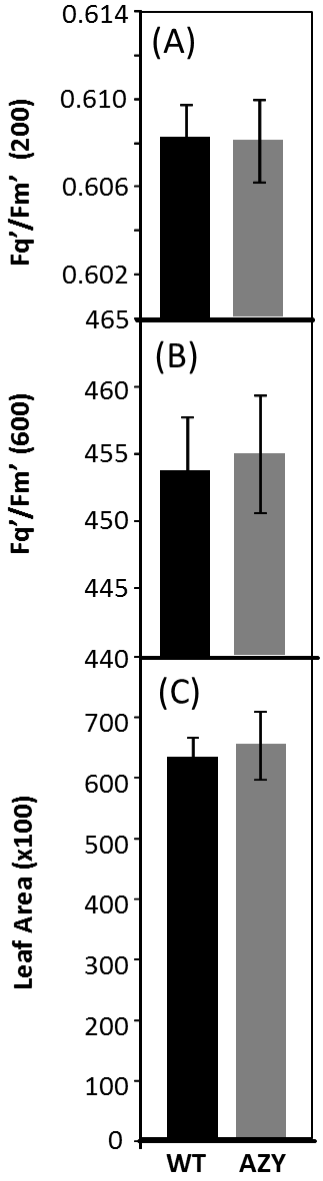

Figure S2. Determination of photosynthetic capacity and leaf area of WT versus azygous (AZY) segregating controls using chlorophyll fluorescence imaging. WT and AZY plants were grown in controlled environment conditions with a light intensity of 130 µmol m^{-2} s^{-1}, 8 h light/16h dark cycle for 14 days and chlorophyll fluorescence imaging used to determine F_q'/F_m' (maximum PSII operating efficiency) at a light intensity of (A) 200 µmol m^{-2} s^{-1}. (B) 600 µmol m^{-2} s^{-1} (The data was obtained using 4 individual plants from each line). (C) leaf area at time of analysis.

(A)

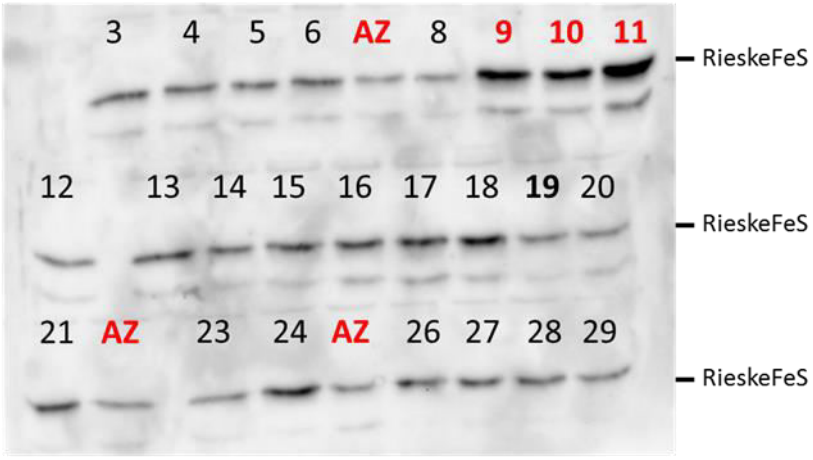

(b)

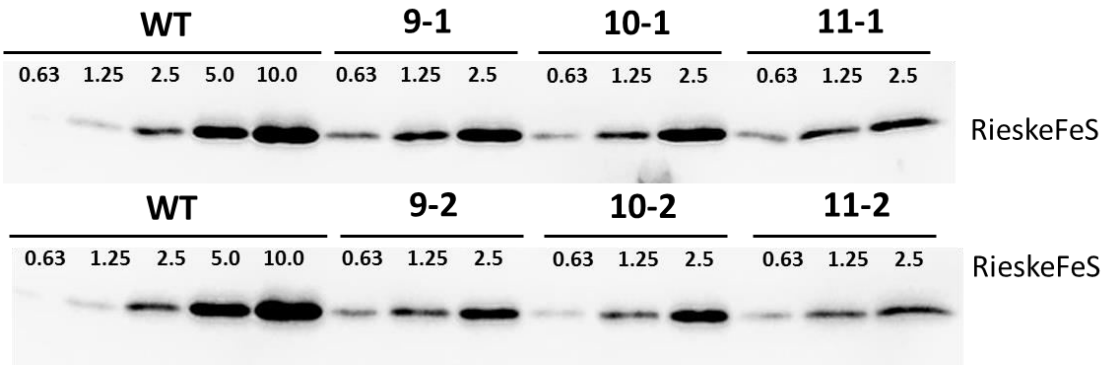

Figure S3. Immunoblot analysis of WT and Rieske FeS ox proteins. (A) Leaf protein extract from leaves from 27 independent T1 transformants. Protein levels were compared to PCR negative lines (AZ). Lines 9, 10 and 11 were selected for further analysis. (B) Protein gradients were loaded for two independent plants per line containing 0.68 to 10µg of protein.

(A)

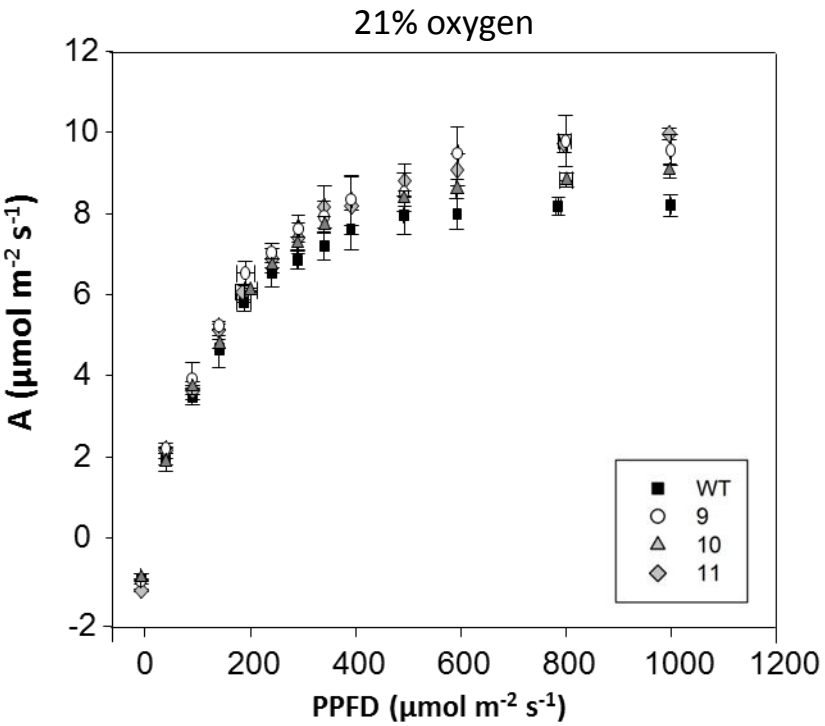

(B)

	A/Q 21% [O_2]			
Name	Light (µmol m^{-2} s^{-1})	F_q'/F_m'	q_P	A_{sat} (µmol m^{-2} s^{-1})
WT	400	0.461 ± 0.012	0.46 ± 0.01	
	1000	0.203 ± 0.006	0.21 ± 0.01	9.9 ± 1.14
9	400	0.478 ± 0.011	0.47 ± 0.06	
	1000	0.220 ± 0.008	0.23 ± 0.01	12.6 ± 0.93
10	400	0.469 ± 0.007	0.47 ± 0.01	
	1000	0.216 ± 0.004	0.22 ± 0.01	12.1 ± 1.2
11	400	0.473 ± 0.003	0.47 ± 0.00	
	1000	0.214 ± 0.006	0.21 ± 0.01	12.3 ± 0.57

Figure S4. Light Response curves of the Rieske FeS plants at 21% [O_2]. (a) Light Response Curves for each Rieske FeS lines compared to wild type (WT). The data was obtained using four individual Rieske FeS ox and WT plants. Standard errors are shown. **(b)** the photosynthetic parameters of WT and Rieske FeS ox lines determined from light response curves (*A*Q) curves

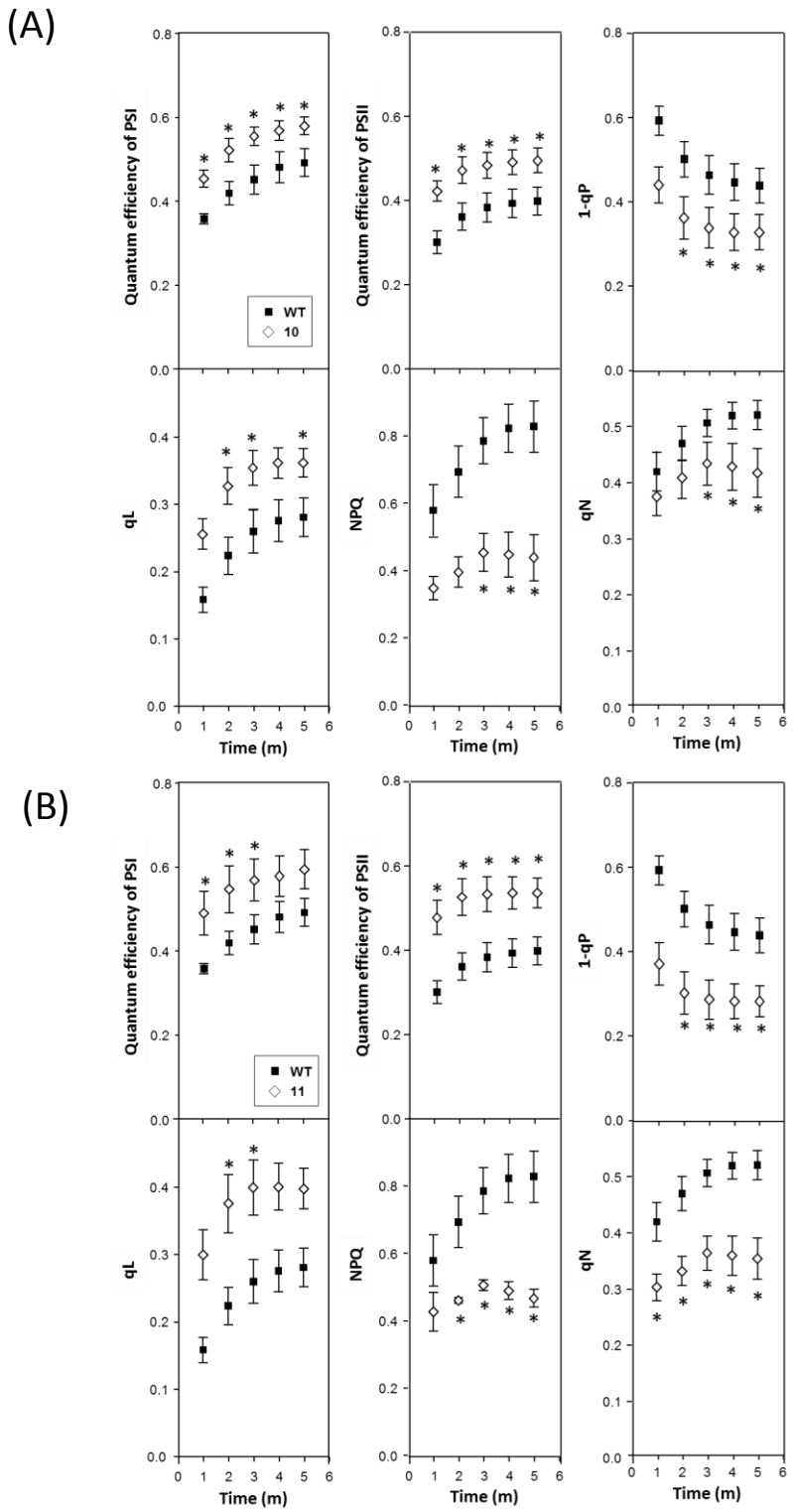

Figure S5. Determination of the efficiency of electron transport in the leaves of mature Rieske Fes ox plants (lines 10 & 11, 34 days after planting). WT and Rieske FeS ox plants were grown in controlled environment conditions with a light intensity of 130 μmol m^{-2} s^{-1}, 8 h light/16 h dark cycle and the redox state was determined using a Dual-PAM at a light intensity of 220 μmol m^{-2} s^{-1}. The data was obtained using four individual plants from Rieske Fes ox line (A) 10 and (B) 11 compared to WT (five plants). Significant differences are indicated (*$p<0.05$). Bars represent Standard errors.

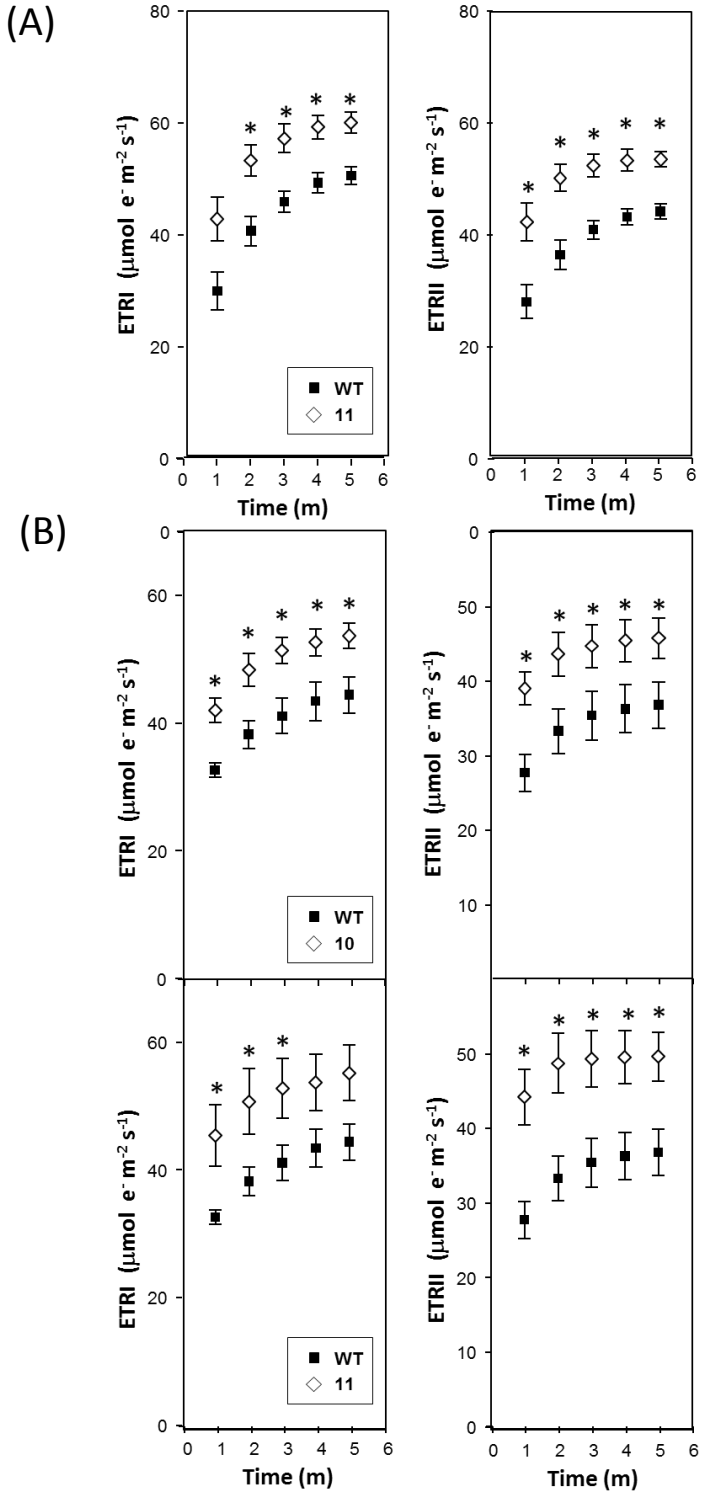

Figure S6. Determination of the efficiency of electron transport in the leaves of (A) young (line 11, (27 days after planting)) and (B) mature Rieske Fes ox plants (lines 10 & 11, (34 days after planting respectively)). WT and Rieske FeS ox plants were grown in controlled environment conditions with a light intensity of 130 µ mol m^{-2} s^{-1}, 8 h light/16 h dark cycle and the redox state was determined using a Dual-PAM at a light intensity of 220 µ mol m^{-2} s^{-1} . The data was obtained using four individual plants from Rieske Fes ox line Significant differences are indicated (*$p<0.05$). Bars represent Standard errors.

Table S1. Physiological parameters of Rieske FeS ox plants compared to WT. The data was obtained using four individual Rieske FeS ox and WT plants. Standard errors are shown.

Plant Type	Abs	F_v/F_m	leaf thickness (μm)
WT	0.878±0.004	0.789 ± 0.006	217 ± 6.2
9	0.873 ± 0.015	0.796 ± 0.009	223 ± 7.5
10	0.876 ± 0.006	0.794 ± 0.007	------
11	0.881 ± 0.003	0.793 ± 0.008	223 ± 2.5